Journal of Alloys and Compounds 509 (2011) 2050–2053

Contents lists available at ScienceDirect

Journal of Alloys and Compounds

journal homepage: www.elsevier.com/locate/jallcom

Current–voltage characteristics of sol–gel derived $SrZrO_3$ thin films for resistive memory applications

Jingxian Wu, Zheng Wen, Di Wu*, Haifa Zhai, Aidong Li

Department of Materials Science and Engineering and National Laboratory of Solid State Microstructures, Nanjing University, Nanjing, Jiangsu 210093, People's Republic of China

ARTICLE INFO

Article history:
Received 27 June 2010
Received in revised form 22 October 2010
Accepted 22 October 2010
Available online 4 November 2010

Keywords:
Thin films
Resistive switching
Sol–gel process

ABSTRACT

$SrZrO_3$ thin films are prepared on $Pt/TiO_2/SiO_2/Si$ substrates by sol–gel process for resistive random access memory applications. The unipolar resistive switching characteristic is achieved in both stoichiometric and Zr-deficient $SrZrO_3$ thin films. Formation and rupture of filaments composed of oxygen vacancies are proposed to explain the observed resistive switching behaviors. By introducing oxygen vacancies into $SrZrO_3$ through making the film Zr-deficient, the conduction mechanism of the high resistance state changes from Ohmic to space charge limited behavior. This may be ascribed to more deep traps associated with oxygen vacancies due to Zr-deficiency. Switching endurance is enhanced significantly in Zr-deficient $SrZrO_3$ due to the reduced Joule heating.

1. Introduction

In the last decade, new types of nonvolatile memories have attracted considerable attention. Non-volatile strategies proposed recently include ferroelectric random access memories (FeRAMs) [1], magnetoresistive random access memories (MRAMs) [2], phase change memories (PCMs) [3] and resistive random access memories (ReRAMs). Among these, ReRAMs have been regarded as promising candidates for the next generation nonvolatile memories due to their simple structure and compatibility with metal oxide semiconductor technologies [4]. The current candidate materials for ReRAM devices include binary transition metal oxides such as ZrO_2 [5], NiO [6], and TiO_2 [7]; perovskite $SrZrO_3$ (SZO) [8–16], ferroelectric $YMn_{1-x}O_3$ [17], Cu doped $Ge_{0.3}Se_{0.7}$ [18].

The ReRAM device can be switched between a low resistance state (LRS or set) and a high resistance state (HRS or reset) after an initial electro-forming step. Switching is referred to as "unipolar" if the set/reset operations can be achieved with the same voltage polarity, as "bipolar" if set/reset operations require opposite voltage polarities. Resistive switching mechanisms consist of a combination of physical and/or chemical effects. These mechanisms can be classified in terms of the dominant contribution: whether it comes from a thermal effect, an electronic effect, or an ionic effect [4]. For unipolar switching, the filament model has been proposed as a possible mechanism [19]. Filaments are created through the insulate matrix during the electroforming process, and are fused as a result of Joule heating by the electric field. It is critical to control the formation and rupture of a filamentary conductive path to improve the resistive switching characteristics.

SZO-based thin films have been studied for ReRAM applications due to its excellent resistive switching properties such as high stability, low operating voltage, high speed, high HRS to LRS resistance ratio, good endurance and long retention time [8,11,12,14,15,20]. Various conduction mechanisms such as Ohmic conduction, space-charge limited conduction (SCLC) and Poole–Frenkel emission were considered in order to explain the dominant conduction mechanisms of the low and high-resistance states in SZO-based ReRAMs [8–16,21]. However, direct experimental demonstrations have not yet been reported to correlate the conduction mechanism with the resistive switching characteristics.

In this study, we compare the conduction behavior and the switching characteristics of stoichiometric and Zr-deficient SZO thin films. Formation and rupture of filaments composed of oxygen vacancies are proposed to explain the observed resistive switching behaviors. The results show that Zr-deficiency may effectively improve the resistive switching characteristics of SZO thin films, probably by introducing more oxygen vacancies.

2. Experimental

100-nm-thick SZO films were deposited by a sol–gel method. The precursor solution was prepared by mixing stoichiometric amount of strontium acetate, zirconium *n*-propoxide dissolved in acetic acid and 2-methoxyethanol, respectively. The precursor solution was then divided into two parts. One is referred to as solution A. The other one was further modified by adding prescribed amount of ammonia to accelerate the hydrolysis of zirconium *n*-propoxide and is referred to as solution B. Both solutions were spin-coated onto $Pt/TiO_2/SiO_2/Si$ substrates at 3000 rpm and then baked at 200 °C on a hot plate for 5 min in air to remove the solvents. The spin-

* Corresponding author. Tel.: +86 25 83621215; fax: +86 25 83594668.
E-mail address: diwu@nju.edu.cn (D. Wu).

0925-8388/$ – see front matter © 2010 Elsevier B.V. All rights reserved.
doi:10.1016/j.jallcom.2010.10.134

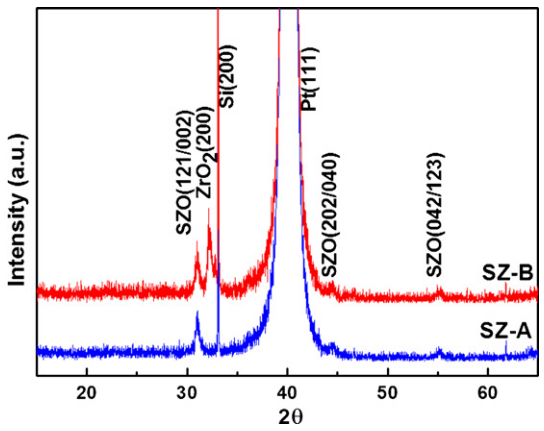

Fig. 1. XRD patterns of SZ-A and SZ-B thin films after 800 °C annealing.

coating and baking procedures were repeated several times to obtain the desired film thickness. The films were then annealed in flowing oxygen at 800 °C for 3 min in a rapid thermal annealing oven. Hereafter, thin films derived from solution A and B are labeled as SZ-A and SZ-B, respectively.

Pt top electrodes of 200 μm in diameter were sputter-deposited through a shadow mask for electrical measurements. These films were characterized by X-ray diffraction (XRD) using a Rigaku Ultima III diffractometer with Cu Kα radiation. A Keithly 2400 sourcemeter was used to measure the current–voltage (*I*–*V*) characteristics of the $SrZrO_3$ capacitors.

3. Results and discussion

Fig. 1 shows the XRD patterns of SZ-A and SZ-B films. SZ-A exhibits a pure perovskite structure [22], while the peak from (2 0 0) crystalline plane of ZrO_2 is observed clearly in the pattern of SZ-B. The formation of ZrO_2 due to the hydrolysis of zirconium *n*-propoxide indicates the presence of Zr-deficiency in the $SrZrO_3$ phase in SZ-B. Therefore, more oxygen vacancies would be expected to compensate additional negative charges in the lattice of $SrZrO_3$.

The reproducible *I*–*V* characteristics of both stoichiometric Pt/SZ-A/Pt and Zr-deficient Pt/SZ-B/Pt capacitors are presented in Fig. 2(a) and Fig. 2(b), respectively. As shown, both of the capacitors exhibit unipolar switching behaviors. After the initial forming process, the capacitors reach a low resistance state (LRS). When sweeping the applied positive voltage to about 1.0 V with a current compliance of 250 mA, a sudden drop of current is observed and the film returns to a high resistance state (HRS). When voltage is swept to about 20.0 V with a current compliance of 5 mA, an abrupt increase of current appears and the LRS is restored. Ten reliable switching cycles including "set" (from HRS to LRS) and "reset" (from LRS to HRS) processes are presented in Fig. 2(a) and (b) for SZ-A and SZ-B respectively. Fig. 2(c) depicts statistics of the forming voltage ($V_{forming}$) and the set voltage (V_{set}) for SZ-A and SZ-B capacitors, respectively, from 10 test cells and 50 tests. Fig. 2(d) shows distributions of the reset voltages (V_{reset}) of both capacitors in 50 tests. No obvious difference is observed between the two capacitors.

Fig. 3 shows the current voltage (*I*–*V*) characteristics of a typical switching cycle redrawn in a log–log plot. In the LRS, both of the two films exhibit Ohmic behavior. This is consistent with those reported previously [10,14,15]. However, the conduction mechanisms of these two samples differ in the HRS. An Ohmic behavior is observed in the HRS of stoichiometric Pt/SZ-A/Pt capacitor, while the *I*–*V* curve in the HRS of Zr-deficient Pt/SZ-B/Pt capacitor shows three distinct regions in the log–log plot. These three *I*–*V* characteristics agree with the Lampert's theory [23], i.e. an Ohmic behavior ($I \sim V$) in the low voltage, a SCLC current following the Child's law ($I \sim V^2$) in the high voltage and a trap-filling limited current ($I \sim V^{\alpha}$) in between.

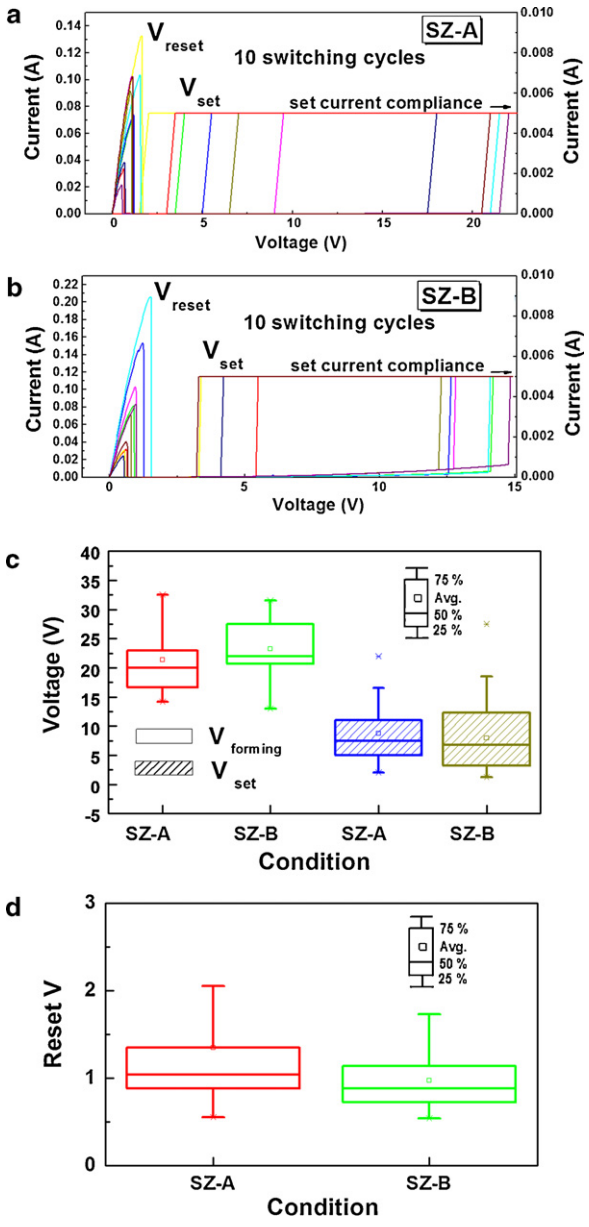

Fig. 2. (a and b) Typical *I*–*V* characteristics of Pt/SZ-A/Pt and Pt/SZ-B/Pt capacitors, respectively. (c and d) Statistics of $V_{forming}$, V_{set} and V_{reset} of Pt/SZ-A/Pt and Pt/SZ-B/Pt capacitors, respectively.

The switching cycling characteristics of both capacitors are shown in Fig. 4. The average ratio between HRS and LRS of both capacitors is larger than 10^4, with the HRS resistance of about 100 kΩ and the LRS resistance of about 10 Ω, respectively. Moreover, the resistance in LRS is independent of the films thickness, compared to our 200 nm-thick films. This is also consistent with those reported recently by Soni et al. [24] and Yang et al. [25]. It is interesting that the Zr-deficient Pt/SZ-B/Pt capacitor keeps stable for up to 600 cycles, 10 times better than that of the stoichiometric Pt/SZ-A/Pt capacitor. Such resistive switching property of SZ-B capacitor exhibits good performance among reported SZO-based devices. [11,14,15,20] The resistive switching of SZO-based memory capacitors in earlier studies is mostly of bipolar character [8–13,15,16,21]. Although Lin et al. [14] reported a unipolar Al/V:SZO-LNO/Pt capacitor, the unipolar characteristic is attributed to the asymmetric electrode materials. However, our Pt/SZO/Pt capacitors have symmetric electrodes and thus asymmetric interface effect cannot lead to the unipolar behavior observed.

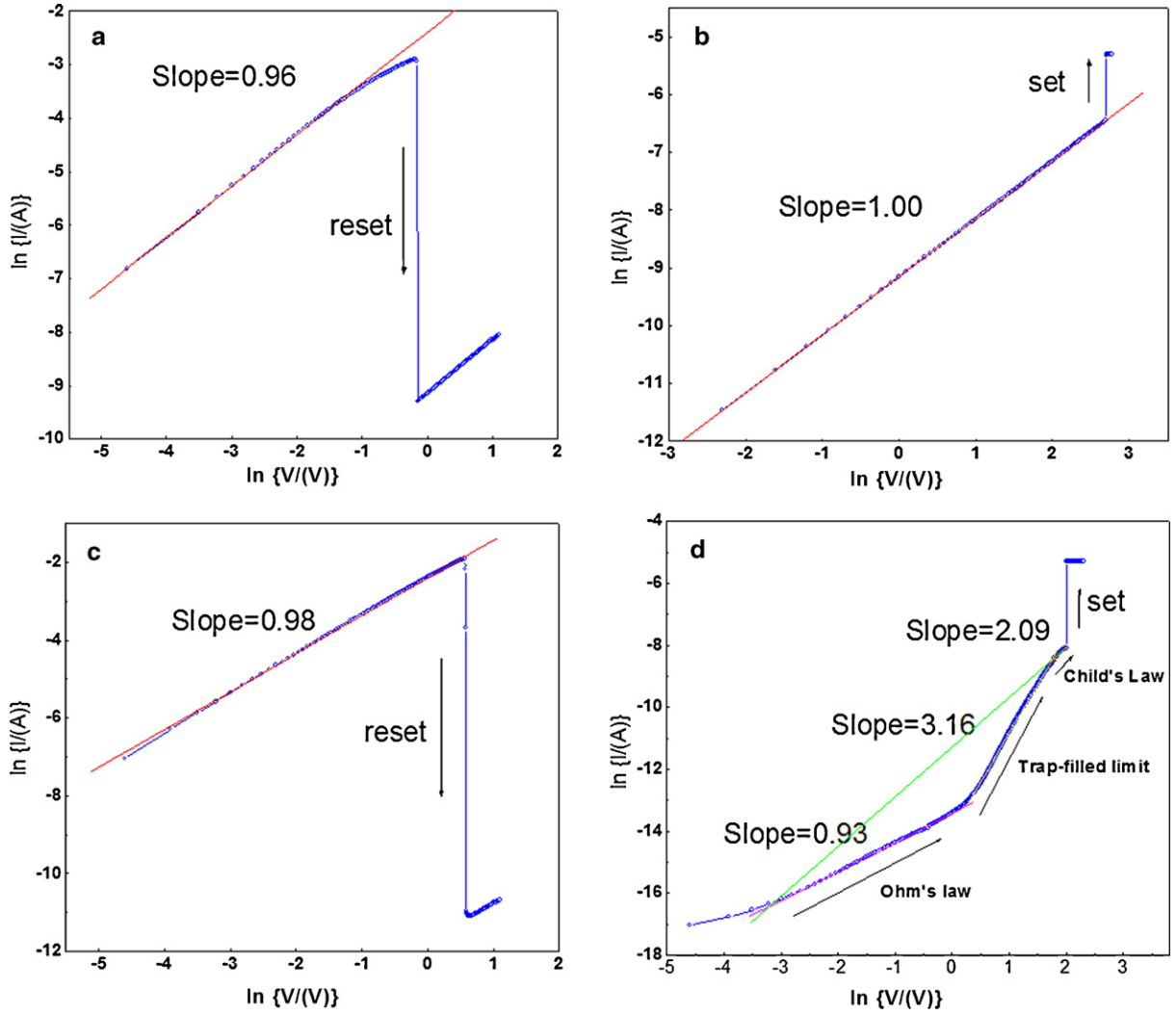

Fig. 3. *I–V* curves in log–log plot. (a) Pt/SZ-A/Pt: from LRS to HRS; (b) Pt/SZ-A/Pt: from HRS to LRS; (c) Pt/SZ-B/Pt: from LRS to HRS and (d) Pt/SZ-B/Pt: from HRS to LRS.

Unipolar resistive switching phenomenon is usually explained by the formation and annihilation of conducting filamentary paths [26]. After an electroforming process, i.e. partial dielectric breakdown initiated by a high voltage, filament in the material would fuse/antifuse by Joule heating [4]. For perovskite oxide thin films, the filament might be composed of oxygen vacancies which are usually the most mobile charged defects in this structure [27]. In the set process, driven by the high electric field, oxygen vacancies can aggregate to form tiny local conducting paths. When the voltage is increased to V_{set}, these tiny local conducting paths may gather to form thicker conducting filaments and the capacitor switches from the HRS to the LRS. In the reset process, oxygen vacancies in the filaments can be dispersed by the electric field with the assistance of Joule heating, leading to localized rupture in these filaments. Consequently, the capacitor switches from the LRS to the HRS. Some filaments, however, may still remain in the HRS.

It is worth noting that stoichiometric SZ-A sample has a higher conductivity in HRS compared to SZ-B sample. In the Ohmic region, SZ-A sample exhibits a higher leakage current than SZ-B sample under the same voltage, as shown in Fig. 3(b) and (d). This indicates that there are more volume-generated free carriers for conduction in SZ-A than SZ-B [23]. It is reported that SCLC is often observed in materials which exhibit a low free charge carrier density [28,29]. Space charge limited effects will not be observed unless the injected free-carrier density, n_j, exceeds the volume-generated free-carrier density, n_0. When n_0 is greater than n_j, the volume conductivity is predominate [23]. This results in an Ohmic behavior, as shown in Fig. 3(b) for the HRS of SZ-A and low-voltage region in Fig. 3(d) for SZ-B. For the SCLC current, the quadratic *I–V* relation indicates shallow traps. However, in Fig. 3(d), the slopes of the log–log plots are greater than 2. This clearly suggests that the SCLC in SZ-B is governed by the exponential trap distribution preferably with deep traps. For Zr-deficient SZ-B, oxygen vacancies may create deep traps [30] that facilitate the SCLC conduction observed.

SCLC conduction mechanism of HRS is often reported in ReRAM materials with bipolar resistive switching behaviors, such as in Au/Cr/Zr^+-implanted-ZrO_2/n^+-Si capacitors [31] and in Ti/ZrO_2/Pt capacitors [32]. SCLC conduction observed in unipolar SZO capacitors implies that oxygen vacancies formed in perovskite SZO matrix are more mobile. Therefore, filaments composed of oxygen vacancies can fuse/antifuse under the same voltage polarity. Moreover, the Pt/SZO/Pt capacitors show the unipolar resistive switching behavior due to the fact that the LRS current reaches the order of 10^{-1} A (Fig. 2(a) and (b)). With the large current flowing through the filaments, the reset process is principally dominated by Joule heating and dispersion of oxygen vacancies (dependent on thermal energy instead of voltage polarity). This phenomenon was also reported previously in unipolar Al/SZO/LNO/Pt capacitors [20].

The switching failure of the capacitor is usually induced by a hard dielectric breakdown. As discussed above, Joule-heating is

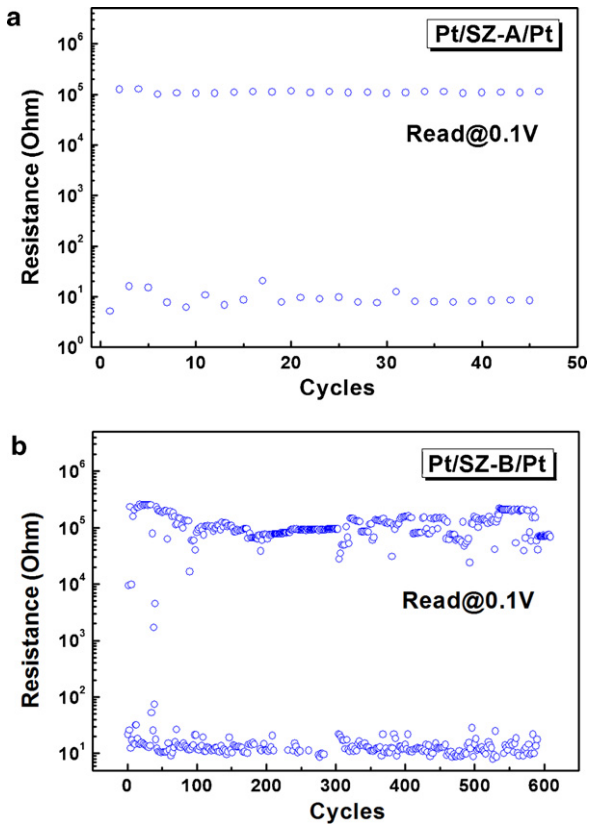

Fig. 4. The switching cycling characteristics of (a) Pt/SZ-A/Pt and (b) Pt/SZ-B/Pt capacitors at room temperature.

widely considered as the driving force for the reset process, i.e., the change from a LRS to a HRS. However, the heat accumulated during the fast cycling would lead to a quick failure since the heat would accelerate the hard dielectric breakdown of the capacitor [25]. As can be seen in Fig. 3(a), the current deviates strongly from the Ohmic behavior when approaching the reset voltage. This phenomenon was also reported previously in unipolar Pt/NiO/Pt resistive switching capacitors [33]. It has been proved that the strong nonlinearity of *I–V* curve in LRS in high voltage region comes from the temperature increase of conducting filaments due to Joule heating. However, this phenomenon is not observed in Fig. 3(c), indicating that Joule heating in Zr-deficient SZ-B sample can be dissipated more easily than in SZ-A. This is consistent with the fact that stoichiometric SZ-A has more free carriers than SZ-B, since the free carrier density should increase with increasing temperature [34].

4. Conclusions

In conclusion, we have shown that the resistive switching properties of $SrZrO_3$ films can be improved by reducing the content of Zr and introducing more oxygen vacancies. Based on the experimental results, the conduction mechanisms in LRS and HRS of Zr-deficient Pt/SZ-B/Pt capacitor are Ohmic and SCLC, respectively. This is different from the stoichiometric Pt/SZ-A/Pt capacitor, which shows Ohmic behavior for both LRS and HRS. The different conduction mechanisms of SZ-A and SZ-B may be attributed to the different amount of oxygen vacancies in the films. Zr-deficiency in SZO also improves the switching life-time. Therefore, the control of the amount of oxygen vacancies may be a major task in ReRAM applications of SZO thin films.

Acknowledgements

This work was jointly sponsored by the Natural Science Foundation of China (Grant Nos. 50872050 and 91022001), the State Key Program for Basic Research of China (Grant No. 2009CB929503).

References

[1] Y. Wang, Z. Wang, H. Xu, D. Li, J. Alloys Compd. 484 (2009) 230–232.
[2] Y.-T. Chen, J.-Y. Tseng, S.-R. Jian, H.-G. Chen, S.-U. Jen, J. Alloys Compd. 485 (2009) 822–825.
[3] Y. Lin, M.H. Hong, G.X. Chen, C.S. Lim, Z.B. Wang, L.S. Tan, L.P. Shi, T.C. Chong, J. Alloys Compd. 449 (2008) 253–257.
[4] R. Waser, M. Aono, Nat. Mater. 6 (2007) 833.
[5] H. Zhang, B. Gao, B. Sun, G. Chen, L. Zeng, L. Liu, X. Liu, J. Lu, R. Han, J. Kang, B. Yu, Appl. Phys. Lett. 96 (2010) 123502.
[6] I. Hwang, M.-J. Lee, G.-H. Buh, J. Bae, J. Choi, J.-S. Kim, S. Hong, Y.S. Kim, I.-S. Byun, S.-W. Lee, S.-E. Ahn, B.S. Kang, S.-O. Kang, B.H. Park, Appl. Phys. Lett. 97 (2010) 052106.
[7] X. Cao, X. Lia, W. Yua, Y. Zhang, R. Yang, X. Liu, J. Kong, W. Shen, J. Alloys Compd. 486 (2009) 458–461.
[8] M.-H. Lin, M.-C. Wu, C.-H. Lin, T.-Y. Tseng, J. Appl. Phys. 107 (2010) 124117.
[9] C.-Y. Liu, P.-H. Wu, A. Wang, W.-Y. Jang, J.-C. Young, K.-Y. Chiu, T.-Y. Tseng, IEEE Electron Device Lett. 26 (2005) 351–353.
[10] J.-W. Park, K. Jung, M.-K. Yang, J.-K. Lee, D.Y. Kim, J.W. Park, J. Appl. Phys. 99 (2006) 124102.
[11] J.-W. Park, J.-W. Park, M.K. Yang, K. Jung, D.-Y. Kim, J.-K. Lee, J. Vac. Sci. Technol. A 24 (2006) 970–973.
[12] C.-C. Lin, B.-C. Tu, C.-C. Lin, C.-H. Lin, T.-Y. Tseng, IEEE Electron Device Lett. 27 (2006) 725–727.
[13] C.-Y. Liu, A. Wang, W.-Y. Jang, T.-Y. Tseng, J. Phys. D: Appl. Phys. 39 (2006) 1156–1160.
[14] C.-C. Lin, C.-Y. Lin, M.-H. Lin, C.-H. Lin, T.-Y. Tseng, IEEE Trans. Electron Devices 54 (2007) 3146–3151.
[15] C.-C. Lin, C.-C. Lin, B.-C. Tu, J.-S. Yu, C.-H. Lin, T.-Y. Tseng, Jpn. J. Appl. Phys. 46 (2007) 2153–2156.
[16] J.-W. Park, M.K. Yang, K. Jung, J.-K. Lee, IEEE Trans. Electron Devices 55 (2008) 1782–1786.
[17] Z.B. Yan, S.Z. Li, K.F. Wang, J.-M. Liu, Appl. Phys. Lett. 96 (2010) 012103.
[18] R. Soni, P. Meuffels, A. Petraru, M. Weides, C. Kügeler, R. Waser, H. Kohlstedt, J. Appl. Phys. 107 (2010) 024517.
[19] S.E. Ahn, M.J. Lee, Y. Park, B.S. Kang, C.B. Lee, K.H. Kim, S. Seo, D.S. Suh, D.C. Kim, J. Hur, W. Xianyu, G. Stefanovich, H. Yin, I.K. Yoo, J.H. Lee, J.B. Park, I.G. Baek, B.H. Park, Adv. Mater. 20 (2008) 924.
[20] M.-H. Lin, M.-C. Wu, C.-Y. Huang, C.-H. Lin, T.-Y. Tseng, J. Phys. D: Appl. Phys. 43 (2010) 295404.
[21] C.-Y. Lin, M.-H. Lin, M.-C. Wu, C.-H. Lin, T.-Y. Tseng, IEEE Electron Device Lett. 29 (2008) 1108–1111.
[22] T. Matsuda, S. Yamanaka, K. Kurosaki, S. Kobayashi, J. Alloys Compd. 351 (2003) 43–46.
[23] M. Lampert, Phys. Rev. 103 (1956) 1648.
[24] R. Soni, P. Meuffels, H. Kohlstedt, C. Kügeler, R. Waser, Appl. Phys. Lett. 94 (2009) 123503.
[25] Y.C. Yang, F. Pan, F. Zeng, New J. Phys. 12 (2010) 023008.
[26] K.M. Kim, B.J. Choi, C.S. Hwang, Appl. Phys. Lett. 90 (2007) 242906.
[27] N. Xu, L.F. Liu, X. Sun, C. Chen, Y. Wang, D.D. Han, X.Y. Liu, R.Q. Han, J.F. Kang, B. Yu, Semicond. Sci. Technol. 23 (2008) 075019.
[28] K.C. Kao, W. Hwang, Electrical Transport in Solids, Pergamon, New York, 1981.
[29] W. Helfrich, P. Mark, Z. Phys. 166 (1962) 370.
[30] X.D. Qi, J. Dho, R. Tomov, M.G. Blamire, J.L. MacManus-Dirscoll, Appl. Phys. Lett. 86 (2005) 062903.
[31] Q. Liu, W. Guan, S. Long, R. Jia, M. Liu, Appl. Phys. Lett. 92 (2008) 012117.
[32] C.-Y. Lin, S.-Y. Wang, D.-Y. Lee, T.-Y. Tseng, J. Electrochem. Soc. 155 (2008) H615.
[33] S.B. Lee, S.C. Chae, S.H. Chang, J.S. Lee, S. Park, Y. Jo, S. Seo, B. Kahng, T.W. Noh, Appl. Phys. Lett. 93 (2008) 252102.
[34] Pradip K.R. Kalita, B.K. Sarma, H.L. Das, Bull. Mater. Sci. 26 (2003) 613–617.